
Message Passing for Collective Graphical Models

Tao Sun¹
Daniel Sheldon^{1,2}
Akshat Kumar³

TAOSUN@CS.UMASS.EDU
SHELDON@CS.UMASS.EDU
AKSHATKUMAR@SMU.EDU.SG

¹University of Massachusetts Amherst, ²Mount Holyoke College, ³Singapore Management University

Abstract

Collective graphical models (CGMs) are a formalism for inference and learning about a population of independent and identically distributed individuals when only noisy aggregate data are available. We highlight a close connection between approximate MAP inference in CGMs and *marginal inference* in standard graphical models. The connection leads us to derive a novel Belief Propagation (BP) style algorithm for collective graphical models. Mathematically, the algorithm is a strict generalization of BP—it can be viewed as an extension to minimize the Bethe free energy plus additional energy terms that are non-linear functions of the marginals. For CGMs, the algorithm is much more efficient than previous approaches to inference. We demonstrate its performance on two synthetic experiments concerning bird migration and collective human mobility.

1. Introduction

In an influential paper, [Yedidia, Freeman, and Weiss \(2000\)](#) showed that the loopy Belief Propagation (BP) algorithm for marginal inference in graphical models can be understood as a fixed-point iteration that attempts to satisfy the first-order optimality conditions of the Bethe free energy, which approximates the true variational free energy. The result shed considerable light on the convergence properties of BP and led to many new ideas for approximate variational inference.

In this paper, we highlight a connection between the Bethe free energy and the objective function for approximate MAP inference in Collective Graphical Models (CGMs) ([Sheldon et al., 2013](#)), which are models for inference and learning about populations when only noisy aggregate data

are available. We then follow reasoning similar to that of [Yedidia et al.](#) to derive a novel message-passing algorithm for CGMs. The algorithm, *non-linear energy belief propagation* (NLBP), has the interesting property that message updates are identical to BP, *with the exception that edge potentials change in each step* based on the gradient of the non-linear “evidence terms” that are present in the CGM objective but not in the Bethe free energy. NLBP is a strict generalization of BP to deal with the presence of these additional non-linear terms.

The new algorithm has significant practical benefits. We show experimentally that, by exploiting the graph structure, NLBP solves the approximate MAP optimization problem for CGMs much faster than a generic optimization solver, and scales significantly better than previous approaches for inference in CGMs. NLBP advances applications of CGMs by significantly reducing the computational burden of inference, which was previously a limiting factor. We demonstrate this point through two synthetic applications. First, we apply CGMs to the problem of modeling bird migration ([Sheldon et al., 2007; 2013; Liu et al., 2014](#)), where inference is used to reconstruct bird migration routes, make forecasts of migration, and learn parameters of migration models. Our algorithm lets us scale from small problems to realistic-sized problems. Second, we contribute a novel application for modeling human mobility ([Candia et al., 2008; Isaacman et al., 2011; 2012](#)). In this case, data providers (e.g., cell phone companies) release aggregate statistics about human movements for the purpose of model fitting, but corrupt those statistics with noise to guarantee differential privacy ([Dwork & Roth, 2013; Mir et al., 2013](#)). CGM inference algorithms provide a way to reason about the true sufficient statistics for the purpose of learning. We show that a CGM-based learning algorithm that uses NLBP is much more accurate than a baseline approach that uses noisy statistics directly for parameter estimation.

2. Collective Graphical Models

CGMs compactly describe the distribution of the aggregate statistics of a population sampled independently from a dis-

crete graphical model. Let $G = (V, E)$ be an undirected graph, and consider the following pairwise graphical model over the discrete random vector $\mathbf{X} = (X_1, \dots, X_{|V|})$:

$$p(\mathbf{x}; \boldsymbol{\theta}) = \Pr(\mathbf{X} = \mathbf{x}; \boldsymbol{\theta}) = \frac{1}{Z(\boldsymbol{\theta})} \prod_{(i,j) \in E} \phi_{ij}(x_i, x_j; \boldsymbol{\theta}). \quad (1)$$

Here, $\phi_{ij}(\cdot, \cdot; \boldsymbol{\theta})$ is a local potential defined on the setting of variables (X_i, X_j) . The local potentials are controlled by a parameter vector $\boldsymbol{\theta}$, and $Z(\boldsymbol{\theta})$ is the partition function. We assume for simplicity that each variable X_i takes values in the same finite set \mathcal{X} . We also assume henceforth that G is a tree. For graphical models that are not trees or have higher-order potentials, our results can be generalized to junction trees, with the usual blowup in space and running-time depending on the clique-width of the junction tree.

Now, consider an ordered sample $\mathbf{x}^{(1)}, \dots, \mathbf{x}^{(M)}$ of random vectors drawn independently from the graphical model. We also refer to this sample as a *population*. Define the contingency tables $\mathbf{n}_i = (n_i(x_i) : x_i \in \mathcal{X})$ over nodes of the model and $\mathbf{n}_{ij} = (n_{ij}(x_i, x_j) : x_i, x_j \in \mathcal{X})$ over edges of the model, whose entries count the number of times particular variable settings occur in the population:

$$\begin{aligned} n_i(x_i) &= \sum_{m=1}^M \mathbb{I}(X_i^{(m)} = x_i), \\ n_{ij}(x_i, x_j) &= \sum_{m=1}^M \mathbb{I}(X_i^{(m)} = x_i, X_j^{(m)} = x_j). \end{aligned}$$

Here, $\mathbb{I}(\cdot)$ is an indicator function. Define the vector \mathbf{n} to be the concatenation of all edge-based contingency tables \mathbf{n}_{ij} together with all node-based contingency tables \mathbf{n}_i . This is a random vector that depends on the entire population and comprises sufficient statistics of the population, which can be seen by writing the joint probability:

$$\begin{aligned} p(\mathbf{x}^{(1)}, \dots, \mathbf{x}^{(M)}; \boldsymbol{\theta}) &= g(\mathbf{n}, \boldsymbol{\theta}) = \\ &= \frac{1}{Z(\boldsymbol{\theta})^M} \prod_{(i,j) \in E} \prod_{x_i, x_j} \phi_{ij}(x_i, x_j; \boldsymbol{\theta})^{n_{ij}(x_i, x_j)}. \quad (2) \end{aligned}$$

In CGMs, one makes noisy observations \mathbf{y} of some subset of the sufficient statistics \mathbf{n} and then seeks to answer queries about the sufficient statistics given \mathbf{y} (e.g., for the purpose of learning the parameters $\boldsymbol{\theta}$) through the conditional distribution $p(\mathbf{n} | \mathbf{y}; \boldsymbol{\theta}) \propto p(\mathbf{n}; \boldsymbol{\theta})p(\mathbf{y} | \mathbf{n})$. The first term in this product, $p(\mathbf{n}; \boldsymbol{\theta})$, is the prior distribution over the sufficient statistics or the *CGM distribution*. In Section 2.2, we will describe how the CGM distribution is derived from the individual model (1). We refer to the second term, $p(\mathbf{y} | \mathbf{n})$, as the *noise model* or the *CGM evidence term*. It is often assumed that $p(\mathbf{y} | \mathbf{n})$ is log-concave in \mathbf{n} , which makes the negative log-likelihood convex in \mathbf{n} , though most of the results of this paper do not rely on that assumption.

Example. For modeling bird migration, assume that $X = (X_1, \dots, X_T)$ is the sequence of discrete locations (e.g. map grid cells) visited by an individual bird, and that the graphical model $p(\mathbf{x}; \boldsymbol{\theta}) = \frac{1}{Z(\boldsymbol{\theta})} \prod_{t=1}^{T-1} \phi_t(x_t, x_{t+1}; \boldsymbol{\theta})$ is a chain model governing the migration of an individual, where the parameter vector $\boldsymbol{\theta}$ controls how different relevant factors (distance, direction, time of year, etc.) influence the affinity $\phi_t(x_t, x_{t+1}; \boldsymbol{\theta})$ between two locations x_t and x_{t+1} . In the CGM, M birds of a given species independently migrate from location to location according to the chain model. The node-table entries $n_t(x_t)$ indicate how many birds are in location x_t at time t . The edge-table entries $n_{t,t+1}(x_t, x_{t+1})$ count how many birds move from location x_t to location x_{t+1} from time t to time $t+1$. A reasonable model for eBird data is that the number of birds of the target species counted by a birdwatcher is a Poisson random variable with mean proportional to the true number of birds $n_t(x_t)$, or $y_t(x_t) | n_t(x_t) \sim \text{Pois}(\alpha n_t(x_t))$, where α is the detection rate. Given only the noisy eBird counts and the prior specification of the Markov chain, the goal is to answer queries about the distribution $p(\mathbf{n} | \mathbf{y}; \boldsymbol{\theta})$ to inform us about migratory transitions made by the population. Because the vector \mathbf{n} consists of sufficient statistics, these queries also provide all the relevant information for learning the parameters $\boldsymbol{\theta}$ from this data.

2.1. CGM Distribution

We now describe the form of the CGM distribution $p(\mathbf{n}; \boldsymbol{\theta})$ and basic aspects of inference in this distribution. [Sundberg \(1975\)](#) originally described the form of this distribution for a graphical model that is decomposable (i.e., its cliques are the nodes of some junction tree), in which case its probabilities can be written in closed form in terms of the marginal probabilities of the original model. [Liu et al. \(2014\)](#) refined this result to be written in terms of the original potentials instead of marginal probabilities. Applied to our tree-structured model, this gives the following CGM distribution:

$$\begin{aligned} p(\mathbf{n}; \boldsymbol{\theta}) &= M! \frac{\prod_{i \in V} \prod_{x_i \in \mathcal{X}} (n_i(x_i)!)^{\nu_i - 1}}{\prod_{(i,j) \in E} \prod_{x_i, x_j \in \mathcal{X}} n_{ij}(x_i, x_j)!} \\ &\cdot g(\mathbf{n}, \boldsymbol{\theta}) \cdot \mathbb{I}(\mathbf{n} \in \mathbb{L}_M^{\mathbb{Z}}). \quad (3) \end{aligned}$$

The first term is a base measure (it does not depend on the parameters) that counts the number of different ordered samples that give rise to the sufficient statistics \mathbf{n} ; in this term, ν_i is the degree of node i . The second term, $g(\mathbf{n}, \boldsymbol{\theta})$, is the joint probability of any ordered sample with sufficient statistics \mathbf{n} as defined in Eq. (2). The final term is a hard constraint that restricts the support of the distribution to vectors \mathbf{n} that are valid sufficient statistics of some ordered sample. [Sheldon & Dietterich \(2011\)](#) showed that, for trees or junction trees, this requirement is satisfied if

and only if \mathbf{n} belongs to the *integer-valued scaled local polytope* $\mathbb{L}_M^{\mathbb{Z}}$ defined by the following constraints:

$$\mathbb{L}_M^{\mathbb{Z}} = \left\{ \mathbf{n} \in \mathbb{Z}_+^{|\mathbf{n}|} \mid M = \sum_{x_i} n_i(x_i) \quad \forall i \in V, \right. \quad (4)$$

$$\left. n_i(x_i) = \sum_{x_j} n_{ij}(x_i, x_j) \quad \forall i \in V, x_i \in \mathcal{X}, j \in N(i) \right\},$$

where $N(i)$ is the set of neighbors of i . The reader will recognize that $\mathbb{L}_M^{\mathbb{Z}}$ is equivalent to the standard local polytope of a graphical model (Wainwright & Jordan, 2008) except for two differences: (1) the marginals, which in our case represent counts instead of probabilities, are scaled to sum to the population size M instead of summing to one, and (2) these counts are constrained to be integers. The set $\mathbb{L}_M^{\mathbb{Z}}$ is the true support of the CGM distribution. Let \mathbb{L}_M be the relaxation of $\mathbb{L}_M^{\mathbb{Z}}$ obtained by removing the integrality constraint, i.e., the set of real-valued vectors with non-negative entries that satisfy the same constraints.

2.2. Approximate MAP Inference

The MAP inference problem for CGMs is to find $\mathbf{n} \in \mathbb{L}_M^{\mathbb{Z}}$ to maximize $p(\mathbf{n} \mid \mathbf{y}; \boldsymbol{\theta})$. Henceforth, we will suppress the dependence on $\boldsymbol{\theta}$ to simplify notation when discussing inference with respect to fixed parameters. Unfortunately, exact MAP inference is intractable (Sheldon et al., 2013), but by relaxing the feasible set from $\mathbb{L}_M^{\mathbb{Z}}$ to \mathbb{L}_M (i.e., removing the integrality requirement), taking the negative log of the objective, and using Stirling’s approximation, Sheldon et al. (2013) arrived at the following convex relaxation of the MAP problem:

$$\min_{\mathbf{z} \in \mathbb{L}_M} F_{\text{CGM}}(\mathbf{z}) := E_{\text{CGM}}(\mathbf{z}) - H_B(\mathbf{z}). \quad (5)$$

$$E_{\text{CGM}}(\mathbf{z}) = - \sum_{(i,j) \in E} \sum_{x_i, x_j} z_{ij}(x_i, x_j) \log \phi_{ij}(x_i, x_j) - \log p(\mathbf{y} \mid \mathbf{z}),$$

$$H_B(\mathbf{z}) = - \sum_{(i,j) \in E} \sum_{x_i, x_j} z_{ij}(x_i, x_j) \log z_{ij}(x_i, x_j) + \sum_{i \in V} (\nu_i - 1) \sum_{x_i} z_i(x_i) \log z_i(x_i).$$

We write \mathbf{z} in place of \mathbf{n} to emphasize that the contingency tables are now real-valued. The quantity $H_B(\mathbf{z})$ is the *Bethe entropy*. It is well known that the Bethe entropy is concave over the local polytope of a tree (Heskes, 2006). We have grouped the remaining terms into the *CGM energy function* $E_{\text{CGM}}(\mathbf{z})$ for comparison with the free energies we will discuss below. If the noise model $p(\mathbf{y} \mid \mathbf{n})$ is log-concave then the overall problem is convex and can be solved by off-the-shelf solvers (Sheldon et al., 2013). This inference approach is extremely accurate and much faster than the previous method of Gibbs sampling, but it is still not efficient enough for large-scale problems.

3. Message Passing Algorithm

The goal of this paper is to derive an efficient special-purpose algorithm to solve the MAP optimization problem. We start by comparing the MAP objective to the *Bethe free energy* for standard graphical models:

$$F_B(\mathbf{z}) = E_B(\mathbf{z}) - H_B(\mathbf{z}),$$

$$E_B(\mathbf{z}) = - \sum_{(i,j) \in E} \sum_{x_i, x_j} z_{ij}(x_i, x_j) \log \phi_{ij}(x_i, x_j).$$

The functions $F_{\text{CGM}}(\mathbf{z})$ and $F_B(\mathbf{z})$ differ only in the energy terms: while the standard energy $E_B(\mathbf{z})$ is linear in \mathbf{z} , the CGM energy $E_{\text{CGM}}(\mathbf{z})$ is non-linear (but typically convex). In what follows, we will generalize the analysis by Yedidia et al. (2000) of Pearl’s classical belief propagation (BP) algorithm (1988) to derive a BP algorithm for arbitrary non-linear energies $E(\mathbf{z})$ such as the one in the CGM MAP objective.

Classical BP maintains a set of messages $\{m_{ij}(x_j)\}$ from nodes to their neighbors, which are updated according to the rule:

$$m_{ij}(x_j) \propto \sum_{x_i} \phi_{ij}(x_i, x_j) \prod_{k \in N(i) \setminus j} m_{ki}(x_i).$$

Upon convergence, the node marginals are $z_i(x_i) \propto \prod_{k \in N(i)} m_{ki}(x_i)$ and the edge marginals are $z_{ij}(x_i, x_j) \propto \phi_{ij}(x_i, x_j) \prod_{k \in N(i) \setminus j} m_{ki}(x_i) \prod_{l \in N(j) \setminus i} m_{lj}(x_j)$, normalized to sum to one. Yedidia et al. (2000) showed that if BP converges, it reaches a zero-gradient point of the Lagrangian of the Bethe free energy with respect to the constraint $\mathbf{z} \in \mathbb{L}_1$, which is the (standard) local polytope. In practice, if BP converges on a loopy graph, it usually converges to a minimum of the Bethe free energy (Heskes, 2003). For trees, BP always converges to the global minimum and the Bethe free energy is equal to the true variational free energy, so BP is an exact method for marginal inference. For graphs with cycles, the Bethe free energy is non-convex and both the Bethe free energy and the constraint set \mathbb{L}_1 are approximations of their counterparts in the exact variational inference problem (Wainwright & Jordan, 2008), so loopy BP is an approximate marginal inference method. A key contribution of Yedidia et al. (2000) was to reveal the nature of this approximation by its connection to the Bethe free energy.

3.1. Non-Linear Energy Belief Propagation

We now present a generalized belief propagation algorithm to solve problems in the form of (5):

$$\min_{\mathbf{z} \in \mathbb{L}_M} F(\mathbf{z}) := E(\mathbf{z}) - H_B(\mathbf{z}), \quad (9)$$

where the energy function $E(\mathbf{z})$ need not be linear with respect to node and edge marginals. As with standard BP,

Algorithm 1: Non-Linear Belief Propagation

Input: Graph $G = (V, E)$, (non-linear) energy function $E(\mathbf{z})$, population size M

Init: $m_{ij}(x_j) = 1$, $\hat{\phi}_{ij}(x_i, x_j) = \phi_{ij}(x_i, x_j)$,
 $z_{ij}(x_i, x_j) \propto \phi_{ij}(x_i, x_j)$, $\forall (i, j) \in E, x_i, x_j$.

while \neg converged **do**

Execute the following updates in any order:

$$\hat{\phi}_{ij}(x_i, x_j) = \exp \left\{ - \frac{\partial E(\mathbf{z})}{\partial z_{ij}(x_i, x_j)} \right\} \quad (6)$$

$$m_{ij}(x_j) \propto \sum_{x_i} \hat{\phi}_{ij}(x_i, x_j) \prod_{k \in N(i) \setminus j} m_{ki}(x_i) \quad (7)$$

$$z_{ij}(x_i, x_j) \propto \hat{\phi}_{ij}(x_i, x_j) \prod_{k \in N(i) \setminus j} m_{ki}(x_i) \prod_{l \in N(j) \setminus i} m_{lj}(x_j) \quad (8)$$

end

Extract node marginals: $z_i(x_i) \propto \prod_{k \in N(i)} m_{ki}(x_i)$

we first present the algorithm and then show the connection to the Lagrangian. Algorithm 1 shows Non-Linear Belief Propagation (NLBP). Note that the *only* difference from standard BP is that we replace the edge potential $\phi_{ij}(x_i, x_j)$ by the exponentiated negative gradient of $E(\mathbf{z})$. For the standard linear energy $E_B(\mathbf{z})$, this is always equal to the original edge potential, and we recover standard BP. For non-linear energies, the gradient is not constant with respect to \mathbf{z} , so, unlike in standard BP, we must track the value of the marginals \mathbf{z} (normalized to sum to M) in each iteration so we can use them to update the current edge potentials. Note that the algorithm stores the current edge potentials $\hat{\phi}_{ij}$ as separate variables, which is not necessary but will add useful flexibility in ordering updates.

One subtle aspect of NLBP is that the vector \mathbf{z} contains redundant information (e.g., edge marginals determine the node marginals) and therefore the gradient of $E(\mathbf{z})$ may depend on details of how that function is defined. For example, consider the two different CGM noise models

$$y_i(x_i) \mid \mathbf{z} \sim \text{Poisson}(\alpha z_i(x_i)),$$

$$y_i(x_i) \mid \mathbf{z} \sim \text{Poisson}\left(\alpha \sum_{x_j} z_{ij}(x_i, x_j)\right).$$

These give the same distribution over \mathbf{y} but yield log-likelihood functions $\log p(\mathbf{y} \mid \mathbf{z})$ (and thus energy functions $E_{\text{CGM}}(\mathbf{z})$) that differ in their gradient with respect to \mathbf{z} . To resolve this ambiguity, we assume that the energy function $E(\mathbf{z})$ (and hence the CGM noise model $p(\mathbf{y} \mid \mathbf{z})$) is always written as a *function of only the edge variables* $\{\mathbf{z}_{ij}\}$. This can be considered a non-linear generalization of the standard practice of absorbing unary node potentials into binary edge potentials in a graphical model, and explains why only the gradient with respect to edge variables appears in the updates of the algorithm.

Theorem 1. Suppose the NLBP message passing updates converge and the resulting vector \mathbf{z} has strictly positive entries. Then \mathbf{z} is a constrained stationary point of $F(\mathbf{z})$ in Problem (9) with respect to the set \mathbb{L}_M . If G is a tree and $E(\mathbf{z})$ is convex, then \mathbf{z} is a global minimum.

Proof. The proof follows Yedidia et al. (2000; 2005). We will write the Lagrangian of (9) and set its gradients to zero to derive the first-order optimality conditions, and then show that these are satisfied by a certain set of Lagrange multipliers if NLBP converges. The Lagrangian is

$$L(\mathbf{z}, \boldsymbol{\lambda}) = E(\mathbf{z}) - H_B(\mathbf{z}) + \sum_i \lambda_i \left(\sum_{x_i} z_i(x_i) - M \right) + \sum_i \sum_{j \in N(i)} \sum_{x_i} \lambda_{ji}(x_i) \left(z_i(x_i) - \sum_{x_j} z_{ij}(x_i, x_j) \right).$$

Since we only consider vectors \mathbf{z} that are strictly positive, we can drop the inequality constraints $\mathbf{z} \geq \mathbf{0}$ when writing the Lagrangian. The partial derivatives with respect to the primal variables are:

$$\frac{\partial L(\mathbf{z}, \boldsymbol{\lambda})}{\partial z_{ij}(x_i, x_j)} = \frac{\partial E(\mathbf{z})}{\partial z_{ij}(x_i, x_j)} + \log z_{ij}(x_i, x_j) + 1 - \lambda_{ji}(x_i) - \lambda_{ij}(x_j),$$

$$\frac{\partial L(\mathbf{z}, \boldsymbol{\lambda})}{\partial z_i(x_i)} = (1 - \nu_i)(\log z_i(x_i) + 1) + \lambda_i + \sum_{j \in N(i)} \lambda_{ji}(x_i).$$

Here we have used the assumption that $E(\mathbf{z})$ depends only on edge variables, so $\frac{\partial E(\mathbf{z})}{\partial z_i(x_i)} = 0$. By setting these expressions to zero and factoring out terms that are constant with respect to the individual edge and node marginal tables, we obtain the following first-order conditions:

$$z_{ij}(x_i, x_j) \propto \exp \left\{ \lambda_{ji}(x_i) + \lambda_{ij}(x_j) - \frac{\partial E(\mathbf{z})}{\partial z_{ij}(x_i, x_j)} \right\},$$

$$z_i(x_i) \propto \exp \left\{ \frac{1}{\nu_i - 1} \sum_{j \in N(i)} \lambda_{ji}(x_i) \right\}. \quad (10)$$

Assume NLBP has converged to a particular set of messages $\{m_{ji}(x_i)\}$ and marginals \mathbf{z} that satisfy Equations (6), (7) and (8). Construct Lagrange multipliers as $\lambda_{ji}(x_i) = \log \left(\prod_{k \in N(i) \setminus j} m_{ki}(x_i) \right)$. By substituting these values into Equations (10) and simplifying the node marginal expression, we obtain the fixed point equations for the marginals from the NLBP algorithm, which are assumed to be satisfied. Therefore, for this set of Lagrange multipliers, the gradient with respect to the primal variables is zero. Finally, it is a standard exercise to check that the normalization and consistency constraints of \mathbf{z} are satisfied when message passing converges, so that the gradient of $L(\mathbf{z}, \boldsymbol{\lambda})$ with respect to $\boldsymbol{\lambda}$ is zero.

This establishes that all partial derivatives of $L(\mathbf{z}, \boldsymbol{\lambda})$ are zero, i.e., \mathbf{z} is an (interior) constrained stationary point. If

G is a tree and $E(\mathbf{z})$ is convex, then the problem is convex and therefore \mathbf{z} must be a global minimum. \square

Note the proof of the theorem does not rely on convexity of the noise term except to guarantee that a global minimum is reached in the case of tree-structured models. Also note that NLBP maintains positive marginals as long as the gradient of $E(\mathbf{z})$ is finite (which is analogous to the assumption of positive potentials in the linear case), so the assumption of positivity is not overly restrictive. Unlike standard BP, which is guaranteed to converge in one pass for trees, in NLBP the edge potentials change with each iteration so it is an open question whether convergence is guaranteed even for trees. In practice, we find it is necessary to damp the updates to messages (Heskes, 2003) and marginals \mathbf{z} , and that sufficient damping always leads to convergence in our experiments. See Algorithm 2 for details of damping.

3.2. Edge Evidence vs. Node Evidence

In our applications we consider two primary types of CGM observations, one where noisy edge counts are observed and one where noisy node counts are observed. In both cases, we assume the table entries are corrupted independently by a univariate noise model $p(y | z)$:

$$p_{\text{edge}}(\mathbf{y} | \mathbf{z}) = \prod_{(i,j) \in E, x_i, x_j} p(y_{ij}(x_i, x_j) | z_{ij}(x_i, x_j)),$$

$$p_{\text{node}}(\mathbf{y} | \mathbf{z}) = \prod_{i, x_i} p(y_i(x_i) | z_i(x_i)).$$

The first model occurs in our human mobility application: a data provider wishes to release *sufficient* statistics (edge tables) but must add noise to those statistics to maintain privacy. The second model occurs in our bird migration application: birdwatchers submit counts that provide evidence only about the locations of birds at a particular time, and not about the migratory transitions they make.

With noisy edge counts, it is clear how to update the edge potentials within NLBP. Let $\ell(z | y) = -\log p(y | z)$. Eq (6) becomes

$$\widehat{\phi}_{ij}(x_i, x_j) = \phi_{ij}(x_i, x_j) \exp \left\{ \ell'(z_{ij}(x_i, x_j) | y_{ij}(x_i, x_j)) \right\},$$

where ℓ' is the partial derivative with respect to the marginal. With noisy node counts, we must rewrite $p(\mathbf{y} | \mathbf{z})$ using only the edge tables. We choose to write $z_i(x_i) = \frac{1}{\nu_i} \sum_{j \in N(i)} \sum_{x_j} z_{ij}(x_i, x_j)$ as the average of the marginal counts obtained from all incident edge tables. This leads to symmetric updates in Eq (6):

$$\widehat{\phi}_{ij}(x_i, x_j) = \phi_{ij}(x_i, x_j) \cdot \exp \left\{ \frac{1}{\nu_i} \ell'(y_i(x_i) | z_i(x_i)) + \frac{1}{\nu_j} \ell'(y_j(x_j) | z_j(x_j)) \right\},$$

where $z_i(x_i)$ and $z_j(x_j)$ are marginal counts of \mathbf{z}_{ij} .

Algorithm 2: Feasibility Preserving NLBP

Input same as Algorithm 1, damping parameter $\alpha \geq 0$

Init : $\mathbf{z} \leftarrow \text{STANDARD-BP}(\{\phi_{ij}\})$

while $\neg \text{converged}$ **do**

$\widehat{\phi}_{ij}(x_i, x_j) \leftarrow \exp \left\{ -\frac{\partial E(\mathbf{z})}{\partial z_{ij}(x_i, x_j)} \right\}, \forall (i, j) \in E$

$\mathbf{z}^{\text{new}} \leftarrow \text{STANDARD-BP}(\{\widehat{\phi}_{ij}\})$

$\mathbf{z} \leftarrow (1 - \alpha)\mathbf{z} + \alpha\mathbf{z}^{\text{new}} ; \quad // \text{damped updates}$

end

3.3. Update Schedules and Feasibility Preservation

The NLBP algorithm is a fixed-point iteration that allows updating of edge potentials, messages, and the marginals in any order. We first considered a *naive schedule*, where message updates are sequenced as in standard BP (for trees, in a pass from leaves to root and then back). When message m_{ij} is scheduled for update, the operations are performed in the order listed in Algorithm 1: first the edge potential is updated, then the message is updated, and then all marginals that depend on m_{ij} are updated. Unlike BP, this algorithm does not achieve convergence in one round, so the entire process is repeated until convergence. In our initial experiments, we discovered that the naive schedule can take many iterations to achieve a solution that satisfies the consistency constraints among marginals (Eq. (4)).

We devised a second *feasibility-preserving schedule* (Algorithm 2) that always maintains feasibility and has the appealing property that it can be implemented as a simple wrapper around standard BP. This algorithm specializes NLBP to alternate between two phases. In the first phase, edge potentials are frozen while messages and marginals are updated in a full pass through the tree. This is equivalent to one call to the standard BP algorithm, which, for trees, is guaranteed to converge in one pass and return feasible marginals. In the second phase, only edge potentials are updated. Algorithm 2 maintains the property that its current iterate \mathbf{z} is always a convex combination of feasible marginals returned by standard BP, so \mathbf{z} is also feasible.

4. Evaluation

We evaluate NLBP with two sets of experiments. First, we evaluate the extent to which NLBP accelerates CGM inference and learning for a benchmark synthetic bird migration problem (Sheldon et al., 2013; Liu et al., 2014). Then, we demonstrate the benefits of a more scalable inference algorithm by evaluating CGMs in a new application: learning with noisy sufficient statistics. We simulate a task where a data provider wishes to release data about human mobility, but must corrupt the data with noise to guarantee privacy.

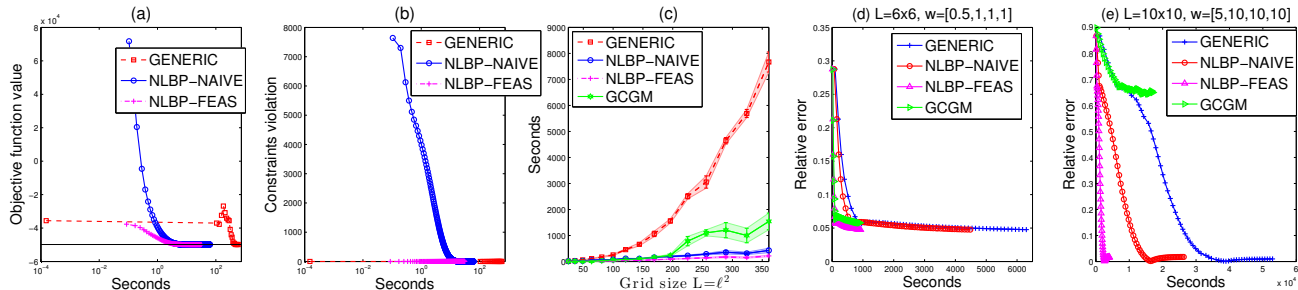


Figure 1. Inference: Comparison of approximate MAP inference algorithms on 15×15 grid: (a) convergence of objective function, (b) convergence of constraint violation, (c) running time vs. number of grid cells (shaded error bars are 95% confidence intervals computed from 15 repeated trials). **Learning:** (d–e) relative error vs. runtime (seconds) for 60 EM iterations and 3 instances; (d) grid size 6×6 and $w_{true} = [0.5, 1, 1, 1]$, (e) grid size 10×10 and $w_{true} = [5, 10, 10, 10]$.

4.1. Speed of Inference: Synthetic Bird Migration

We compared the speed and accuracy of NLBP both as a standalone inference method and as a subroutine for learning versus the baselines of using MATLAB’s interior-point algorithm to solve the approximate MAP problem (Sheldon et al., 2013) and inference in the Gaussian approximation of CGMs (Liu et al., 2014).

Following (Sheldon et al., 2013; Liu et al., 2014), synthetic data is generated from a chain-structured CGM to simulate migration of a population of M birds from the bottom-left corner to the top-right corner of an $\ell \times \ell$ grid. Each bird makes independent migration decisions. The transition probability between cells x_t and x_{t+1} comes from a logistic regression formula that employs several covariates: the distance from x_t to x_{t+1} , the consistency of transition direction with wind direction, the consistency of the transition direction with the intended destination, and the preference of the individual to move. The individual model is a T -step Markov chain with variable X_t indicating the cell location in the grid. The cardinality of variable X_t is $L = \ell^2$. Let w denote the parameters in the logistic regression. We report results for $w_{true} = (5, 10, 10, 10)$. The results for other parameter settings (e.g., those from Liu et al. (2014)) were very similar. After generating node and edge contingency tables \mathbf{n} from this process, we added Poisson noise $y \sim \text{Pois}(\alpha n)$ to the nodes, with detection rate $\alpha = 1$. In the following experiments, we set $M = 1000$, $T = 20$ and vary grid size L from 5×5 to 19×19 .

Inference. We compared MATLAB’s interior point solver (GENERIC), NLBP with the naive message schedule (NLBP-NAIVE), feasibility-preserving NLBP (NLBP-FEAS), and the Gaussian approximation (GCGM) for performing inference in CGMs.

Figures 1(a–b) show the convergence behavior of the first three algorithms, which solve the same approximate MAP problem, in terms of both objective function and constraint violation for $L = 15 \times 15$. The objective value of the

two NLBP algorithms converges to the optimum an order of magnitude more quickly than the generic solver. Both GENERIC and NLBP-FEAS maintain feasibility, but NLBP-NAIVE takes a long time to achieve feasibility—much longer than it does to converge to the optimal objective value. Since GCGM takes a different approach to inference, we do not evaluate it directly in terms of the objective and constraints of the approximate MAP problem. However, we note that when either the grid size or parameter values are large, GCGM produces marginals that violate the consistency constraints, which may explain why it has difficulty in parameter learning in these cases (see below).

Figure 1(c) shows the total time to convergence as a function of problem size for all four algorithms. Both NLBP variants are very efficient and their running times scale much better than that of GENERIC. NLBP-FEAS is approximately twice as fast as NLBP-NAIVE, and is approximately four times faster than GCGM.

Learning. Approximate MAP inference is an effective subroutine within the E-step of an expectation maximization (EM) algorithm for learning CGM parameters (Sheldon et al., 2013). We compared the speed and accuracy of EM using the four different approximate MAP algorithms as subroutines. We generated data by fixing parameters w_{true} and generating three independent realizations of the entire bird migration process ($T = 20$) to simulate observing the seasonal migration of the same species across three different years. Each realization had different wind covariates, and was treated within EM as an independent data instance.

We used approximate MAP inference for the E-step and a gradient-based solver to update the parameters w in the M-step. For EM details, see (Sheldon et al., 2013; Liu et al., 2014). We evaluated the performance in terms of the relative error, defined as $\|w^{(t)} - w_{true}\|_1 / \|w_{true}\|_1$, where $w^{(t)}$ are the parameters from the t -th EM iteration. Figures 1(d–e) show the reduction in error over 60 EM iterations for each algorithm on 6×6 and 10×10 grids. The

results confirm the speed advantages of NLBP over the generic solver. All algorithms converge to a similar level of error, except for GCGM in the larger grid size and parameter setting, which is consistent with the results for inference. Both NLBP variants converge much more quickly than GENERIC. The speed advantage of NLBP-FEAS over NLBP-NAIVE is even greater within the EM procedure. GCGM is only competitive for the setting with small grid size and parameter values.

4.2. Human Mobility

We now turn to a novel application of CGMs. We address the problem of learning the parameters of a chain-structured graphical model for human mobility, where, unlike the bird migration model, we have access to *transition counts* (edge counts) instead of node counts. Transition counts are sufficient statistics for the model, so learning with *exact* transition counts would be straightforward. However, we assume the available data are corrupted by noise to maintain privacy of individuals. The problem becomes one of learning with noisy sufficient statistics.

In particular, our application simulates the following situation: a mobile phone carrier uses phone records to collect information about the transitions of people among a discrete set of regions, for example, the areas closest to each mobile tower, which form a Voronoi tessellation of space (Song et al., 2010; de Montjoye et al., 2013). Data is aggregated into discrete time steps to provide hourly counts of the number of people that move between each pair of regions. The provider wishes to release this aggregate data to inform public policy and scientific research about human mobility. However, to maintain the privacy of their customers, they choose to release data in a way that maintains the privacy guarantees of *differential privacy* (Dwork & Roth, 2013; Mir et al., 2013). In particular, they follow the Laplace mechanism and add independent Laplace noise to each aggregate count (Dwork & Roth, 2013).

Ground-Truth Model. We are interested in fitting models of daily commuting patterns from aggregate data of this form. We formulate a synthetic version of this problem where people migrate among the grid cells of a 15×14 rectangular map. We simulate movement from home destinations to work destinations across a period of $T = 10$ time steps (e.g., half-hour periods covering the period from 6:00 a.m. to 11:00 a.m.). We parameterize the joint probability of the movement sequence for each individual as:

$$p(\mathbf{x}_{1:10}) = \frac{1}{Z} \cdot \phi_1(x_1) \cdot \left(\prod_{t=1}^9 \psi(x_t, x_{t+1}) \right) \cdot \phi_{10}(x_{10}).$$

The potentials ϕ_1 and ϕ_{10} represent preferences for home and work locations, respectively, while ψ is a pairwise potential that scores transitions as more or less preferred. For

the ground truth model, we use compact parameterizations for each potential: ϕ_1 and ϕ_{10} are discretized Gaussian potentials (that is, $\phi(x_t)$ is the value of a Gaussian density over the map measured at the center of grid cell x_t) centered around a “residential area” (top right of the map) and “commercial area” (bottom left). For the transition potential, we set $\phi(x_t, x_{t+1})$ proportional to $\exp(-\|v_t - v_{t+1}\|^2 / (2\sigma^2))$, where v_t and v_{t+1} are the centers of grid cells x_t and x_{t+1} , to prefer short transitions over long ones.

Data Generation. To generate data, we simulated $M = 1$ million trajectories from the ground truth model, computed the true transition counts, and then added independent Laplace noise to each true count n to generate the noisy count y . The Laplace noise is controlled by a scale parameter b :

$$p(y | n) = \text{Laplace}(b; n) = \frac{1}{2b} \exp\left\{-\frac{|y - n|}{b}\right\}.$$

To explore the relative power of edge counts versus node counts for model fitting, we also performed a version of the experiments where we marginalized the noisy transition counts to give only noisy node counts $y_t(x_t) = \sum_{x_{t+1}} y_{t,t+1}(x_t, x_{t+1})$ as evidence.

Parameters and Evaluation. We wish to compare the abilities of CGM-based algorithms and a baseline algorithm to recover the true mobility model. When *fitting* models, it would be a severe oversimplification to assume the simple parametric form used to generate data. Instead, we use a fully parameterized model with parameters $\theta = (\log \phi_1, \log \phi_{10}, \log \psi)$. Here $\log \phi_1$ and $\log \phi_{10}$ are arbitrary $L \times 1$ vectors, and $\log \psi$ is an arbitrary $L \times L$ table. Note that this parameterization is over-complete, and hence not identifiable. To evaluate fitted models, we will compare their *pairwise marginal distributions* to those of the ground truth model: unlike the potentials, the pairwise marginals uniquely identify the joint distribution. The pairwise MAE is defined as the mean absolute error among all $L^2 \times (T - 1)$ entries of the pairwise marginals. We also considered node MAE, which is the mean error among the $L \times T$ entries of the node marginals. Note that these *do not* uniquely identify the distribution, but node MAE is an interesting metric for comparing the ability to learn with node evidence vs. edge evidence.

Algorithms. Is it possible to estimate parameters of a graphical model given only noisy sufficient statistics? An “obvious” approach is to ignore the noise and perform maximum-likelihood estimation using the noisy sufficient statistics \mathbf{y} in place of the true ones \mathbf{n} . To the best of our knowledge, this is the only previously available approach, and we use it as a baseline. The approach has been criticized in the context of general multidimensional contingency tables (Yang et al., 2012). To maximize the like-

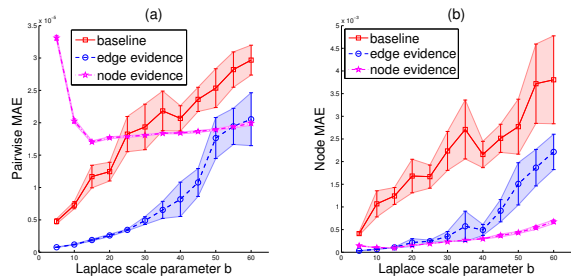


Figure 2. Pairwise / Node MAE vs Laplace scale parameter b after 250 EM iterations. Shaded regions shows 95% confidence intervals computed from 10 trials for each setting.

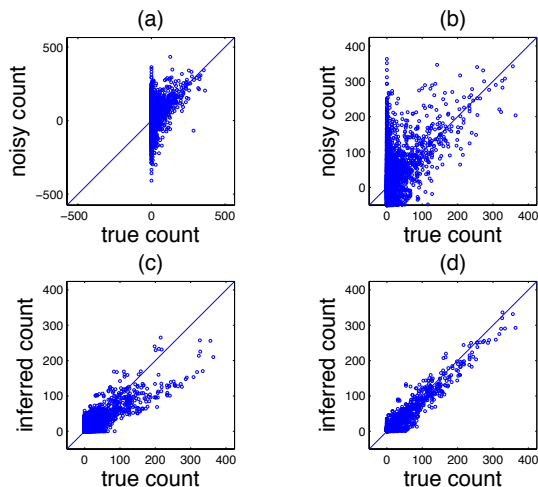


Figure 3. Scatter plots of approximate vs. true edge counts for a small problem ($L = 4 \times 7, T = 5, M = 10000, b = 50$): (a) original noisy edge counts, (b) shown only in the same range as (c-d) for better comparison, (c) reconstructed counts after 1 EM iteration, (d) reconstructed counts after EM convergence.

likelihood with respect to our parameters, we use a gradient-based optimizer with message passing as a subroutine to compute the likelihood and its gradient (Koller & Friedman, 2009).

For the CGM-based approach, we treat the true sufficient statistics as hidden variables and use EM to maximize the likelihood. The overall EM approach is the same as in the bird migration model. When the evidence is noisy edge counts, we first run the baseline algorithm and use those parameters to initialize EM. When the evidence is noisy node counts, the baseline algorithm does not apply and we initialize the parameters randomly.

Results. Figure 2(a) shows the quality of the fitted models (measured by pairwise MAE) vs. the scale of the Laplace noise. For the CGM-based algorithms, we ran 250 EM iterations, which was enough for convergence in almost all cases. Initializing EM with the baseline parameters

helped achieve faster convergence (not shown). The results demonstrate that the CGM algorithm with edge evidence improves significantly over the baseline for all values of b . As expected, the node evidence version of the CGM algorithm performs worse, since it has access to less information. However, it is interesting that the CGM with only node evidence outperforms the baseline (which has access to more information) for larger values of b .

Figure 2(b) shows *node* MAE vs b for the same fitted models. In other words, it measures the ability of the methods to find models that match the ground truth on single time-step marginals. We see that both CGM algorithms are substantially better than the baseline, and the CGM algorithm with *less information* (node counts only) performs slightly better. We interpret this as follows: node evidence alone provides enough information to match the ground truth model on node marginals; the additional information of the noisy edge counts helps narrow the model choices to one that also matches the ground truth edge marginals. However, this does not explain why the node evidence performs *better* than edge evidence for node MAE. We leave a deeper investigation of this for future work—it may be a form of implicit regularization.

Figure 3 provides some insight into the EM algorithm and its ability to reconstruct edge counts. The original, noisy counts have considerable noise and sometimes take negative values (panels (a) and (b)). After one EM iteration (panel (c)), the reconstructed counts are now feasible, so they can no longer be negative, and they are closer to the original counts. After EM converges, the reconstructed counts are much more accurate (panel (d)).

5. Conclusion

This paper highlights a close connection between the problems of approximate MAP inference in collective graphical models (CGMs) and marginal inference in standard graphical models. Inspired by this connection, we derived the non-linear belief propagation (NLBP) algorithm and presented a feasibility-preserving version of NLBP that can be implemented as a simple wrapper around standard BP. By applying NLBP to a synthetic benchmark problem for bird migration modeling, we showed that NLBP runs significantly faster than a generic solver and is significantly more accurate than inference in the Gaussian approximation of CGMs when the grid size or parameter values are large. The feasibility-preserving version of NLBP is twice as fast as the naive NLBP. We then demonstrated the utility of the NLBP algorithm by contributing a novel application of CGMs for modeling human mobility. In this application, CGMs provide a way to fit graphical models when the available sufficient statistics have been corrupted by noise to maintain the privacy of individuals.

Acknowledgments

This material is based upon work supported by the National Science Foundation under Grant No. 1125228, and by the National Research Foundation Singapore under its Corp Lab@University scheme.

References

- Candia, Julián, González, Marta C, Wang, Pu, Schoenharl, Timothy, Madey, Greg, and Barabási, Albert-László. Uncovering individual and collective human dynamics from mobile phone records. *Journal of Physics A: Mathematical and Theoretical*, 41(22):224015, 2008.
- de Montjoye, Yves-Alexandre, Hidalgo, César A, Verleyesen, Michel, and Blondel, Vincent D. Unique in the crowd: The privacy bounds of human mobility. *Scientific reports*, 3, 2013.
- Dwork, Cynthia and Roth, Aaron. The algorithmic foundations of differential privacy. *Theoretical Computer Science*, 9(3-4):211–407, 2013.
- Heskes, T. Convexity arguments for efficient minimization of the Bethe and Kikuchi free energies. *Journal of Artificial Intelligence Research*, 26(1):153–190, 2006.
- Heskes, Tom. Stable fixed points of loopy belief propagation are minima of the Bethe free energy. *Advances in Neural Information Processing Systems (NIPS)*, 15: 359–366, 2003.
- Isaacman, Sibren, Becker, Richard, Cáceres, Ramón, Kobourov, Stephen, Martonosi, Margaret, Rowland, James, and Varshavsky, Alexander. Ranges of human mobility in Los Angeles and New York. In *IEEE International Conference on Pervasive Computing and Communications Workshops (PERCOM Workshops)*, pp. 88–93, 2011.
- Isaacman, Sibren, Becker, Richard, Cáceres, Ramón, Martonosi, Margaret, Rowland, James, Varshavsky, Alexander, and Willinger, Walter. Human mobility modeling at metropolitan scales. In *Proceedings of the 10th international conference on Mobile systems, applications, and services*, pp. 239–252. ACM, 2012.
- Koller, D. and Friedman, N. *Probabilistic graphical models: principles and techniques*. MIT press, 2009.
- Liu, Li-Ping, Sheldon, Daniel, and Dietterich, Thomas G. Gaussian approximation of collective graphical models. In *International Conference on Machine Learning (ICML)*, volume 32, pp. 1602–1610, 2014.
- Mir, Darakhshan J, Isaacman, Sibren, Cáceres, Ramón, Martonosi, Margaret, and Wright, Rebecca N. Dp-where: Differentially private modeling of human mobility. In *IEEE International Conference on Big Data*, pp. 580–588, 2013.
- Pearl, Judea. *Probabilistic reasoning in intelligent systems: networks of plausible inference*. Morgan Kaufmann, 1988.
- Sheldon, Daniel, Elmohamed, M. A. S., and Kozen, Dexter. Collective inference on Markov models for modeling bird migration. In *Advances in Neural Information Processing Systems (NIPS)*, pp. 1321–1328, 2007.
- Sheldon, Daniel, Sun, Tao, Kumar, Akshat, and Dietterich, Thomas G. Approximate inference in collective graphical models. In *International Conference on Machine Learning (ICML)*, volume 28, pp. 1004–1012, 2013.
- Sheldon, Daniel R and Dietterich, Thomas G. Collective graphical models. In *Advances in Neural Information Processing Systems (NIPS)*, pp. 1161–1169, 2011.
- Song, Chaoming, Qu, Zehui, Blumm, Nicholas, and Barabási, Albert-László. Limits of predictability in human mobility. *Science*, 327(5968):1018–1021, 2010.
- Sundberg, R. Some results about decomposable (or Markov-type) models for multidimensional contingency tables: distribution of marginals and partitioning of tests. *Scandinavian Journal of Statistics*, 2(2):71–79, 1975.
- Wainwright, M.J. and Jordan, M.I. Graphical models, exponential families, and variational inference. *Foundations and Trends in Machine Learning*, 1(1-2):1–305, 2008.
- Yang, Xiaolin, Fienberg, Stephen E, and Rinaldo, Alessandro. Differential privacy for protecting multidimensional contingency table data: Extensions and applications. *Journal of Privacy and Confidentiality*, 4(1): 5, 2012.
- Yedidia, Jonathan S, Freeman, William T, and Weiss, Yair. Generalized belief propagation. In *Advances in Neural Information Processing Systems (NIPS)*, volume 13, pp. 689–695, 2000.
- Yedidia, Jonathan S, Freeman, William T, and Weiss, Yair. Constructing free-energy approximations and generalized belief propagation algorithms. *IEEE Transactions on Information Theory*, 51(7):2282–2312, 2005.